Journal of Ovarian Research

RESEARCH

Open Access

Nicotinamide riboside supplementation ameliorates ovarian dysfunction in a PCOS mouse model

Zhenye Zhu[1,2,3], Min Lei[1,2,3], Ruizhi Guo[1,2,3], Yining Xu[1,2,3], Yanqing Zhao[1,2,3], Chenlu Wei[1,2,3], Qingling Yang[1,2,3*] and Yingpu Sun[1,2,3*]

Abstract

Polycystic ovary syndrome (PCOS) is the leading cause of anovulatory infertility among women of reproductive age, yet the range of effective treatment options remains limited. Our previous study revealed that reduced levels of nicotinamide adenine dinucleotide (NAD^+) in ovarian granulosa cells (GCs) of women with PCOS resulted in the accumulation of reactive oxygen species (ROS) and mitochondrial dysfunction. However, it is still uncertain whether increasing NAD^+ levels in the ovaries could improve ovarian function in PCOS. In this study, we demonstrated that supplementation with the NAD^+ precursor nicotinamide riboside (NR) prevented the decrease in ovarian NAD^+ levels, normalized estrous cycle irregularities, and enhanced ovulation potential in dehydroepiandrosterone (DHEA)-induced PCOS mice. Moreover, NR supplementation alleviated ovarian fibrosis and enhanced mitochondrial function in ovarian stromal cells of PCOS mice. Furthermore, NR supplementation improved oocyte quality in PCOS mice, as evidenced by reduced abnormal mitochondrial clustering, enhanced mitochondrial membrane potential, decreased ROS levels, reduced spindle abnormality rates, and increased early embryonic development potential in fertilized oocytes. These findings suggest that supplementing with NAD^+ precursors could be a promising therapeutic strategy for addressing ovarian infertility associated with PCOS.

Keywords Nicotinamide adenine dinucleotide, Nicotinamide riboside, Polycystic ovary syndrome, Ovary, Mitochondrial, Fibrosis

Graphical Abstract

Ovarian NAD^+ levels decreased in DHEA-induced PCOS mice, accompanied by mitochondrial dysfunction in oocytes and ovarian stromal cells, resulting in reduced oocyte quantity and quality, decreased early embryonic development potential, and increased ovarian fibrosis. After increasing ovarian NAD^+ levels by NR supplementation to restore PCOS-related impairment of mitochondria function, ovarian dysfunction in PCOS was attenuated as characterized by improved oocyte quantity and quality, enhanced early embryonic development potential, and decreased ovarian fibrosis.

*Correspondence:
Qingling Yang
qingling531@163.com
Yingpu Sun
syp2008@vip.sina.com
Full list of author information is available at the end of the article

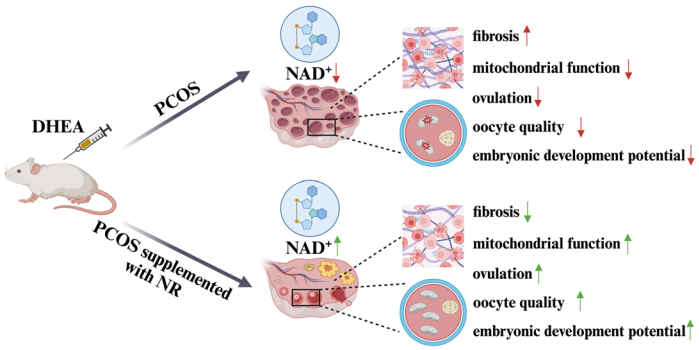

Introduction

During reproductive years, polycystic ovary syndrome (PCOS) is considered a primary contributor to hyperandrogenemia and oligo-anovulation [1]. It is distinguished by the arrest of antral follicle development before reaching the mature, preovulatory stage [2, 3]. However, clinical treatments for PCOS-related ovarian infertility primarily rely on lifestyle adjustments and assisted reproductive technologies (ART) [4, 5]. Although the precise etiology of PCOS remains incompletely understood, recent studies have implicated mitochondrial abnormalities in the pathogenesis and progression of ovarian dysfunction and fibrosis associated with PCOS [6–9].

The initial documentation of increased ovarian stromal proliferation and collagenization in PCOS patients suggested a correlation between PCOS and ovarian fibrosis [10]. Moreover, impaired mitochondrial function in ovarian stromal cells emerges as a pivotal factor in stromal inflammation and fibrosis [11], potentially impeding normal follicle growth and release [12–14]. Mitochondrial dysfunction, characterized by impaired adenosine triphosphate (ATP) production, altered mitochondrial dynamics, and increased production of reactive oxygen species (ROS) [15], leads to oxidative stress—an imbalance between ROS production and antioxidant defenses [16]. This cascade triggers inflammation and apoptosis, facilitating fibroblast activation and extracellular matrix protein deposition in the ovarian stroma [17–19]. Furthermore, compromised mitochondrial bioenergetics exacerbate fibrotic processes within the ovaries of PCOS patients [20]. Previous studies have highlighted mitochondrial dysfunction in both oocytes and granulosa cells (GCs) from women with PCOS [21, 22], emphasizing its significant contribution to PCOS pathogenesis. Therefore, targeted improvement of mitochondrial function emerges as a pivotal therapeutic approach for addressing PCOS-associated ovarian infertility.

However, in vivo evidence regarding the correlation between ovarian dysfunction related to PCOS and nicotinamide adenine dinucleotide (NAD^+) levels remains inadequately substantiated. NAD^+, an important coenzyme coupled with redox reactions [23], maintains mitochondrial function. Additionally, NAD^+ is involved in regulating the activity of various enzymes [24], including those closely related to mitochondrial function, such as the Sirtuins family [25], further influencing mitochondrial biological functions. Our previous research observed a decrease in NAD^+ levels in ovarian granulosa cells from women with PCOS, while supplementation with NAD^+ precursor, nicotinamide riboside (NR), ameliorated mitochondrial dysfunction in Lipopolysaccharide (LPS)-treated human granulosa-like tumor cell line (KGN) [22]. Furthermore, the decline in NAD^+ levels and ovarian dysfunction with age was mitigated by NR supplementation, as evidenced by previous studies [26, 27]. However, whether NR supplementation could ameliorate ovarian dysfunction in PCOS remains uncertain.

Here, we established the PCOS mouse model through DHEA treatment. We found that NR supplementation reduced the decline in ovarian NAD^+ levels, alleviated the disrupted estrous cycles, enhanced the ovulation potential, and reduced the rate of abnormal oocytes in PCOS mice. NR supplementation also enhanced oocyte quality in PCOS mice, evidenced by reduced abnormal mitochondrial clustering, increased mitochondrial membrane potential, decreased ROS levels, lower spindle abnormality rates, and improved early embryonic developmental potential in oocytes post-fertilization. Furthermore, NR supplementation mitigated ovarian fibrosis in

PCOS mice through the improvement of mitochondrial function within ovarian stromal cells. These results indicated that NAD^+ precursor supplementation might offer a promising therapeutic approach for addressing ovarian infertility associated with PCOS.

Materials and methods

Animals

Approval for animal studies was obtained from the ethics committee. Female ICR mice were obtained from SPF (Beijing) Biotechnology Co., Ltd. Standard conditions were maintained for housing, including unrestricted access to food and water, a controlled environment with appropriate temperature and humidity, and a 12-h light–dark cycle. As previously mentioned [28–30], the female mice aged 3 weeks were subcutaneously injected with 60 mg DHEA/kg body weight (MCE, USA) dissolved in 0.2 ml of sesame oil (MCE, USA) to induce the PCOS mouse model, while the control mice received a daily injection of 0.2 ml sesame oil. After 21 days of DHEA treatment, the injections were discontinued, and DHEA-treated mice were randomly assigned to two experimental groups. One group received NR (Jiangsu Medicience Biological Medicine Co., Ltd) supplementation at a dose of 400 mg/kg/day for a period of 14 days, while the other group maintained a standard diet. This dose was selected based on previous studies, which demonstrated that it effectively increased NAD^+ levels and improved mitochondrial function [26, 31–34]. At the end of the 14-day intervention, all three groups of mice were processed simultaneously and under identical experimental conditions.

NAD^+ content detection

For the assessment of ovarian NAD^+ levels, we utilized the NAD^+/NADH assay Kit (Abcam, UK). The procedure involved lysing ovaries in buffer, followed by centrifugation to obtain the supernatant. To this supernatant, 25 µl of NAD^+ extraction buffer was added and incubated at 37 °C for 15 min. Subsequently, a mixture comprising 25 µl of NADH extraction buffer and 75 µl of NAD^+/NADH reaction mix was introduced. The mixture was then incubated for 2 h at room temperature in darkness. Total NAD^+ levels were quantified using the Varioskan Flash Multimode Reader (Thermo Fisher Scientific, USA) via colorimetric analysis, with excitation and emission wavelengths set at 540 nm and 590 nm, respectively.

NAD^+ levels in ovarian stromal cells were quantified using the NAD^+/NADH Quantification Kit (Sigma Aldrich, USA). The procedure involved harvesting and lysing the cells in NADH/NAD^+ extraction buffer, followed by centrifugation to obtain the supernatant. To this supernatant, 100 µl of the master reaction mix was added and incubated at room temperature for 5 min. Subsequently, 10 µl of NADH developer was introduced, and the mixture was incubated in darkness at room temperature for 4 h. The absorbance was then determined at 450 nm using the microplate reader (Thermo Fisher Scientific, USA).

Ovarian ATP content detection

Ovarian ATP content was measured using the ATP Assay Kit (Beyotime, China). In brief, 100 µl of ATP detection lysis buffer was added to each ovary, followed by ultrasonic homogenization. The homogenates were then centrifuged at 12000 g for 5 min at 4 °C, and the supernatant was collected and stored on ice for further use. Subsequently, 100 µl of ATP detection working solution was added to each well and incubated at room temperature for 5 min. Then, 20 µl of the sample or standard was added to each well. Finally, the relative light units (RLU) or counts per minute (CPM) were measured using a luminometer or liquid scintillation counter.

Estrous cycle and histological analysis

Estrous cycle monitoring, as detailed previously [35], involved a two-week analysis of vaginal cytology. Phosphate-buffered saline (PBS) was employed for vaginal douching and harvesting exfoliated vaginal cells. These cells, suspended in PBS, were evenly spread onto slides, air-dried, and then subjected to fixation using 95% ethanol. Subsequent to hematoxylin and eosin (H&E) staining, a microscopic examination of the slides was conducted utilizing an optical microscope (Nikon, Japan). Ovaries were harvested from three distinct groups of mice during diestrus and 15 h post-human chorionic gonadotropin (hCG) treatment. The tissues were fixed overnight in 4% (w/v) paraformaldehyde at 4 °C, then embedded in paraffin. Sectioned of 5 µm thick slices were prepared and subjected to H&E staining. An optical microscope (Nikon, Japan) was used for the analysis of these stained sections.

Oocytes collection and ROS levels detection

Oocyte collection was performed via ovulation induction in mice from the three experimental groups. The protocol involved an intraperitoneal injection of 7.5 IU pregnant mare serum gonadotropin (PMSG), followed by 7.5 IU hCG 47.5 h later. Cumulus-oocyte complexes (COCs) were harvested from the oviductal ampullae 15 h post-hCG administration. To obtain denuded oocytes, the COCs were treated with 0.1% hyaluronidase (Sigma Aldrich, USA). ROS levels were quantified using ROS assay kits. Metaphase II (MII) oocytes collected from three different groups of mice were incubated with MitoSOX™ Red reagent (Thermo Fisher Scientific, USA)

under conditions of 37 °C and 5% CO_2 for 30 min. Following incubation, the oocytes underwent three washes in the M2 medium. Oocyte images were acquired using the Zeiss LSM 700 Confocal laser scanning microscope (Germany). ROS levels were quantified by analyzing the fluorescence intensity using Image J software.

Mitochondrial distribution and mitochondrial membrane potential (ΔΨm) assessment

For the analysis of mitochondrial distribution, MII oocytes from three groups of mice were incubated with MitoTracker™ Red (Invitrogen, USA) at 37 °C and 5% CO_2 for 30 min. Following incubation, the oocytes underwent three washes in the M2 medium. The mitochondrial distribution within these oocytes was subsequently examined using the Zeiss LSM 700 Confocal laser scanning microscope (Germany). The oocytes were then categorized based on the presence of normal or aberrant mitochondrial distribution. Mitochondrial membrane potential (ΔΨm) was assessed in MII oocytes from the three experimental groups. Oocytes were incubated with JC-1 (Beyotime, China) at 37 °C and 5% CO_2 for 30 min, then washed thrice in the M2 medium. Images were captured using the Zeiss LSM 700 Confocal laser scanning microscope (Germany). The fluorescence intensity was quantified using Imaging J software, with the ΔΨm expressed as the ratio of red to green fluorescent pixels.

Spindle assembly analysis

Oocytes from three groups were initially collected, followed by fixation in 4% paraformaldehyde containing 0.5% Triton X-100 for 30 min to allow permeabilization. Subsequent to fixation, the oocytes underwent a blocking step with 1% BSA for 20 min. They were then subjected to an overnight incubation at 4 °C with an anti-α-tubulin antibody (Sigma Aldrich, USA). Following this, a series of washes with 1% BSA was performed thrice, after which the oocytes were subjected to incubation with anti-mouse 488 fluorescent secondary antibody (Invitrogen, USA) droplets at 37 °C for 1 h. Another round of three washes with 1% BSA ensued. The oocytes were then transferred to 10 μl of antifade mounting medium with DAPI (Vector, USA). Spindle morphology and chromosome alignment were visualized and analyzed using the Zeiss LSM 700 Confocal laser scanning microscope (Germany).

In vitro fertilization (IVF) and embryo culture

Male ICR mice aged 4 months were euthanized to extract spermatozoa from dissected epididymides, which were then suspended in an HTF culture medium (Nanjing Aibei Biotechnology, China). Following a 1-h capacitation period at 37 °C and 5% CO_2, the spermatozoa were diluted to a concentration of $1–5\times10^6$/ml and introduced into IVF fertilization medium (COOK, New Zealand). The fertilization process was carried out at 37 °C and 5% CO_2 for 6 h. Oocytes exhibiting two pronuclei post-fertilization were considered successfully fertilized and subsequently transferred to the KSOM culture medium (Nanjing Aibei Biotechnology, China). Over the course of the following 4 days, the rates of 2-cell embryo formation and blastocyst development were observed.

PSR staining

Picrosirius Red Staining (PSR) was performed using a Picrosirius Red Stain Kit (Polysciences, USA) according to the manufacturer's protocol. Sections were sequentially treated with solution A (phosphomolybdic acid) for 2 min at room temperature, followed by solution B (Picrosirius Red F3BA Stain) for 1 h. After washing with solution C (0.1 N hydrochloric acid), slides were dehydrated in 70% alcohol and mounted in neutral resin. Images were captured using a Nikon optical microscope (Japan). Ovarian fibrosis quantification was conducted using Image J software. Images were converted to 8-bit, and a threshold was established based on DHEA-treated mice ovarian staining. This threshold was consistently applied across all groups. The fibrosis area was determined by normalizing staining intensity to stromal areas, excluding follicles and corpora lutea.

Immunohistochemistry staining

Paraffin-embedded ovarian sections were deparaffinized by washing twice with 100% xylene, followed by rehydration through a graded series of alcohol solutions and a brief wash in distilled water. Antigen retrieval was carried out by heating the sections in sodium citrate buffer (pH 6.0) at 95 °C for 15 min. After antigen retrieval, the sections were permeabilized and blocked with 1% BSA containing 0.5% Triton X-100 for 1 h at room temperature. The primary antibody, Anti-alpha smooth muscle actin (Abcam, UK), was applied and incubated overnight at 4 °C. Following a PBS wash, horseradish peroxidase-conjugated secondary antibodies (ZSGB-BIO, China) were applied. For visualization, 3,3'-diaminobenzidine (DAB) chromogen (ZSGB-BIO, China) was used to develop the color. The sections were counterstained with hematoxylin, followed by dehydration through a graded series of alcohols, and cleared in 100% xylene. Finally, the sections were mounted with a resinous mounting medium and cover slipped. The stained sections were observed and analyzed under a Nikon optical microscope (Japan).

Isolation of stromal cells

Ovaries retrieved from each mouse were collected 15 h post-hCG injection. Utilizing insulin needles under a

microscope, corpora lutea and follicles were meticulously removed, leaving behind residual ovarian tissue. These remaining tissues were then transferred to an L15 medium (Thermo Fisher Scientific, USA) supplemented with 0.1% collagenase (Sigma Aldrich, USA) and subjected to incubation at 37 °C and 5% CO_2 for 30 min with agitation every 5 min. Following this, stromal cells were isolated using 40 μm filters (Biologix, China) and subsequently centrifuged at 2000 rpm for 5 min. The absence of significant expression of granulosa cell (*Fshr*) and oocyte (*Bmp15*) markers was confirmed (Fig. 4D and E).

RNA isolation and quantitative real-time PCR

Total RNA was extracted from ovarian stromal cells using the RNeasy Mini Kit (Qiagen, Germany), and cDNA synthesis was performed with HiScript III RT SuperMix for qPCR (Vazyme, China). Quantitative real-time PCR was conducted using a CFX96 Touch Deep Well Real-Time PCR Detection System (BIO-RAD, USA) with ChamQ Universal SYBR qPCR Master Mix (Vazyme, China). Primer sequences are listed in Table S2. All experiments were performed in triplicate. Gene expression levels were calculated using the ΔCT method and normalized to *Gapdh*.

Detection of ROS levels and mitochondrial membrane potential in stromal cells

Ovarian stromal cells were treated with MitoSOX™ Red reagent (Thermo Fisher Scientific, USA) for 30 min at 37 °C and 5% CO_2. After three washes with pre-heated PBS buffer, a minimum of 10,000 cells were examined to determine ROS levels by flow cytometry (FCM). For the evaluation of mitochondrial membrane potential, ovarian stromal cells were exposed to JC-1 (Beyotime, China) for 30 min at 37 °C and 5% CO_2. After three washes with pre-heated PBS buffer, at least 10,000 cells were scrutinized to assess mitochondrial membrane potential by FCM.

Statistical analysis

Statistical analysis was performed using GraphPad Prism 9.0 (GraphPad Software, USA). The experimental design included distinct groups of mice, with data collected from individual mouse ovaries or pooled cells from multiple mice, as detailed in the figure legends. Each measurement was derived from separate samples. Data are presented as mean ± SD. Comparative analyses among the Control, DHEA, and DHEA + NR supplementation groups were conducted using one-way ANOVA. The purity of stromal cell isolation was evaluated using Student's *t*-test. Statistical significance was defined as $P < 0.05$.

Results

NR supplementation improved ovarian function in PCOS mice

To induce the mouse model of PCOS, DHEA was injected subcutaneously for 21 days, with sesame oil treatment serving as the control, as shown in Fig. 1A. Body weight monitoring across the two groups revealed increased weight gain in the DHEA-treated group (Fig. S1A). To evaluate the potential improvement of ovarian function in PCOS mice through NAD^+ precursor supplementation, NR was administered in the diet of DHEA-treated mice for 2 weeks at a dose of 400 mg/kg/day (Fig. 1A). Analysis showed no statistically significant difference in ovarian weight among the three groups (Fig. S1B and C). Notably, ovaries from DHEA-treated mice exhibited decreased NAD^+ levels and NAD^+/NADH ratios compared to controls (Fig. 1B and D). However, NR supplementation increased ovarian NAD^+ levels and NAD^+/NADH ratios in DHEA-treated mice (Fig. 1B and D), indicating that NR supplementation alleviated the decline in ovarian NAD^+ levels and maintained the NAD^+/NADH redox balance in PCOS mice. In addition, we observed a significant decrease in ATP content in the ovaries of DHEA-treated mice (Fig. 1E). However, following NR supplementation, ovarian ATP levels were notably increased (Fig. 1E). We also evaluated the mRNA expression levels of mitochondrial respiratory complex-related genes in the ovaries of three groups of mice by qRT-PCR. The results showed that ovarian mRNA expression levels of *Ndufv1* (Complex I), *Sdhb* (Complex II), *Uqcrc2* (Complex III), and *Atp5a1* (Complex V) were significantly

(See figure on next page.)

Fig. 1 NR supplementation increased ovarian NAD^+ levels and improved ovulatory function in PCOS mice. **A** Diagram of DHEA-induced PCOS mouse model and NR supplementation. **B** NAD^+ levels, **C** NADH levels, and (**D**) the ratios of NAD^+/NADH in the ovaries of three groups of mice ($n = 5$ mice for each group). **E** Relative ovarian ATP content in three groups of mice ($n = 5$ mice for each group). **F** Transcriptional levels of *Ndufv1*, *Sdhb*, *Uqcrc2*, and *Atp5a1* genes in the ovaries were measured by qRT-PCR ($n = 3$ replicates from 3 mice). **G** Estrous cycles in three groups of mice ($n = 4$ mice for each group). M, metestrus; D, diestrus; P, proestrus; E, estrus. **H** Representative images of MII oocytes from three groups of mice. Abnormal oocytes with cytoplasmic fragments were indicated by arrows. Scale bar, 100 μm. **I** Number of ovulated oocytes from three groups of mice ($n = 8$ mice for each group). **J** Percentages of abnormal oocytes from three groups of mice ($n = 8$ mice for each group). **K** H&E-stained gonadotropin-treated ovary sections from three groups of mice, with arrows indicating magnified corpora lutea or unruptured follicles. Scale bar, 500 μm. The panels a-c showed high-magnification images of the specified regions. Scale bar, 100 μm. Data are presented as the mean ± SD. $^*P < 0.05$, $^{**}P < 0.01$, and $^{***}P < 0.001$ by one-way ANOVA compared to DHEA-treated mice

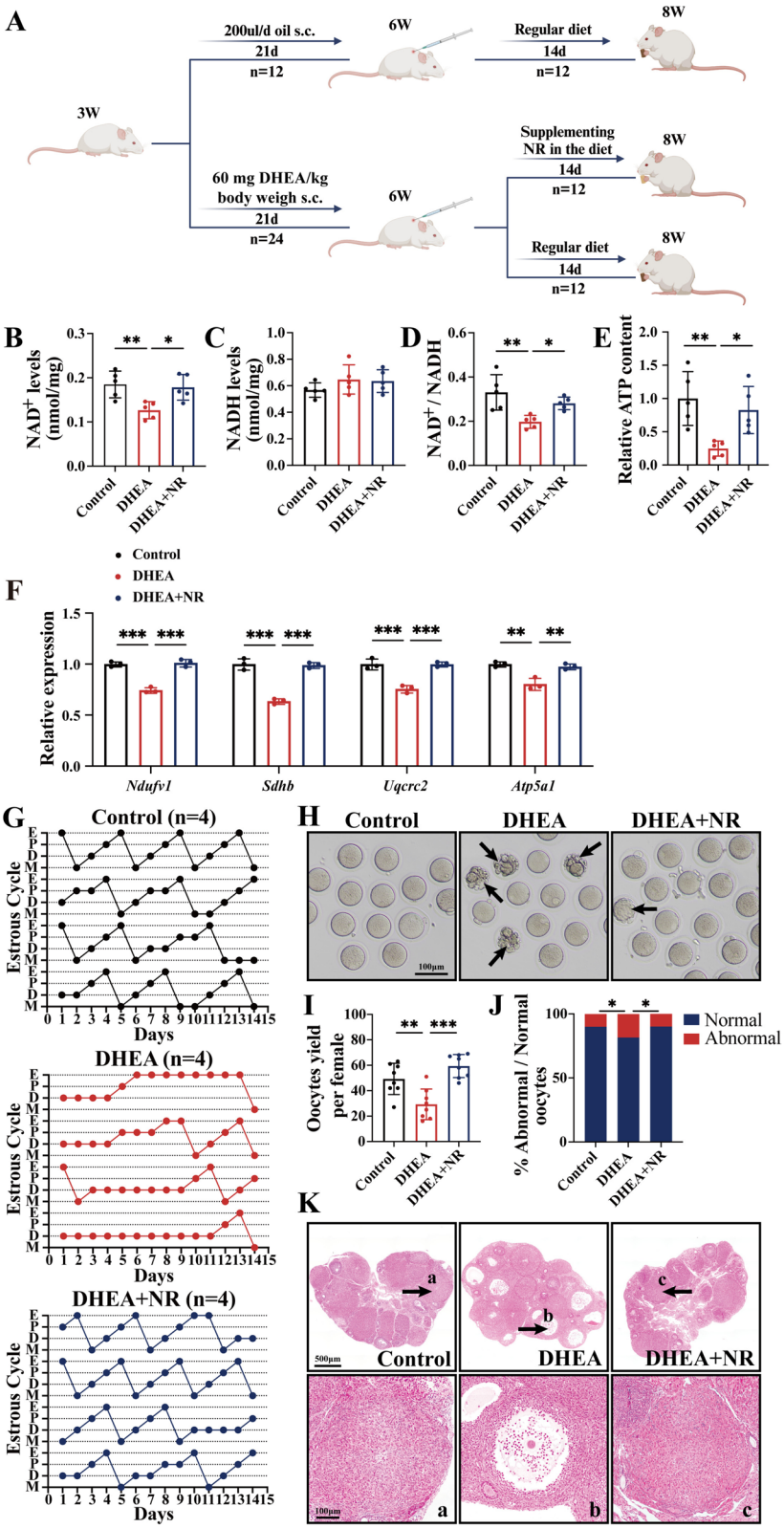

Fig. 1 (See legend on previous page.)

reduced in DHEA-treated mice compared with controls (Fig. 1F). Following NR supplementation, these genes were significantly upregulated (Fig. 1F). These results suggested that NR supplementation improved ovarian mitochondrial function and energy metabolism in DHEA-induced PCOS mice.

The estrous cycle was monitored to assess the effects of DHEA and/or NR on ovarian function. We found that NR supplementation restored the disrupted estrous cycle (extended diestrus and estrus) in the DHEA-treated mice, which exhibited a regular 4–5-day estrus cycle like that of controls (Fig. 1G). Following ovulation induction with gonadotropins, mice treated with DHEA exhibited a significant decrease in the number of ovulated oocytes compared to controls (Fig. 1H and I). This decrease was also accompanied by a higher incidence of abnormal oocyte morphology, characterized by an increase in fragmented oocytes (Fig. 1H and J). In contrast, NR supplementation increased the number of oocytes to about twofold higher than that of the DHEA-treated mice and decreased the rate of fragmented oocytes (Fig. 1H-J). Gonadotropin-treated ovary sections from controls and DHEA + NR-treated mice exhibited multiple corpora lutea (Fig. 1K and Fig. S1D). In contrast, sections from DHEA-treated mice displayed large unruptured follicles (Fig. 1K and Fig. S1D). This observation suggested that NR supplementation improved ovulatory function in PCOS mice.

NR supplementation improved oocyte quality in PCOS mice

Considering that oxidative stress is a critical factor in the pathogenesis of PCOS [36], ROS content was detected by MitoSOX staining. Quantitative analysis revealed that the ROS content in oocytes from DHEA-treated mice was approximately 1.6 times higher than that in controls (Fig. 2A and B). However, supplementation with NR significantly reduced the ROS accumulation in oocytes of DHEA-treated mice (Fig. 2A and B), indicating that oxidative damage in oocytes of PCOS mice could be alleviated by NR supplementation. Mitochondria are a primary ROS source, while excessive ROS accumulation leads to mitochondrial dysfunction [37–39]. Therefore, we further assessed whether NR supplementation could improve mitochondrial function in the oocytes of PCOS mice. MitoTracker staining showed an increase in abnormal mitochondrial aggregated clusters in MII oocytes from DHEA-treated mice compared to controls (Fig. 2C and D), while NR supplementation significantly reduced the percentage of oocytes with an abnormal mitochondrial distribution (Fig. 2C and D). In addition, we monitored the mitochondrial membrane potential by JC-1 staining. Quantitative analysis indicated that the mitochondrial membrane potential in MII oocytes from DHEA-treated mice was lower than that of controls, as evidenced by the decreased ratio of red to green fluorescence intensity (Fig. 2E and F). However, NR supplementation effectively increased the mitochondrial membrane potential (Fig. 2E and F). These results indicated that supplementing with NR improved oocyte quality in PCOS mice by reducing ROS content and improving mitochondrial function.

NR supplementation enhanced early embryonic development potential in PCOS mice

Considering the close association between spindle assembly and oxidative stress in oocytes [40, 41], spindle morphology of MII oocytes from three groups of mice was examined. To visualize the spindles, anti-α-tubulin antibody staining was employed, while chromosome localization was determined using DAPI staining. MII oocytes from the control group exhibited a standard barrel-shaped spindle morphology with chromosomes precisely aligned on the equatorial plate (Fig. 3A and B). Conversely, DHEA-treated mice showed a higher proportion of MII oocytes with atypical spindle morphology, such as disorganized or elongated spindles, and improperly aligned chromosomes (Fig. 3A and B). However, after NR supplementation, the meiotic defects observed in MII oocytes were mitigated (Fig. 3A and B). Given that meiotic abnormalities in oocytes reduce early embryonic development potential after fertilization [42, 43], we next performed IVF of MII oocytes from three groups of mice. We found that DHEA-induced PCOS mice exhibited decreased rates of 2-cell embryos and blastocyst formation compared to controls (Fig. 3C and D). As expected, supplementation with NR to DHEA-treated mice increased the rates of 2-cell embryos and blastocyst formation (Fig. 3C and D). Taken together, these results suggested that NR supplementation could reduce oocyte meiotic defects and enhance the early embryonic development potential of PCOS mice.

NR supplementation reduced ovarian fibrosis in PCOS mice

Ovarian fibrosis is associated with PCOS, which may affect follicle development and ovulation [11, 44]. To investigate whether NR supplementation could alleviate ovarian fibrosis in PCOS mice, we evaluated the ovarian collagen I/III content across the three groups using PSR staining, a recognized indicator of fibrosis. Quantitative analysis revealed increased ovarian fibrosis in DHEA-induced PCOS mice compared to controls, as evidenced by a higher percentage of PSR-positive areas in ovarian sections (Fig. 4A and B). However, NR supplementation significantly reduced the accumulation of ovarian fibrillar collagen in PCOS mice (Fig. 4A and B). We also performed immunohistochemical staining of

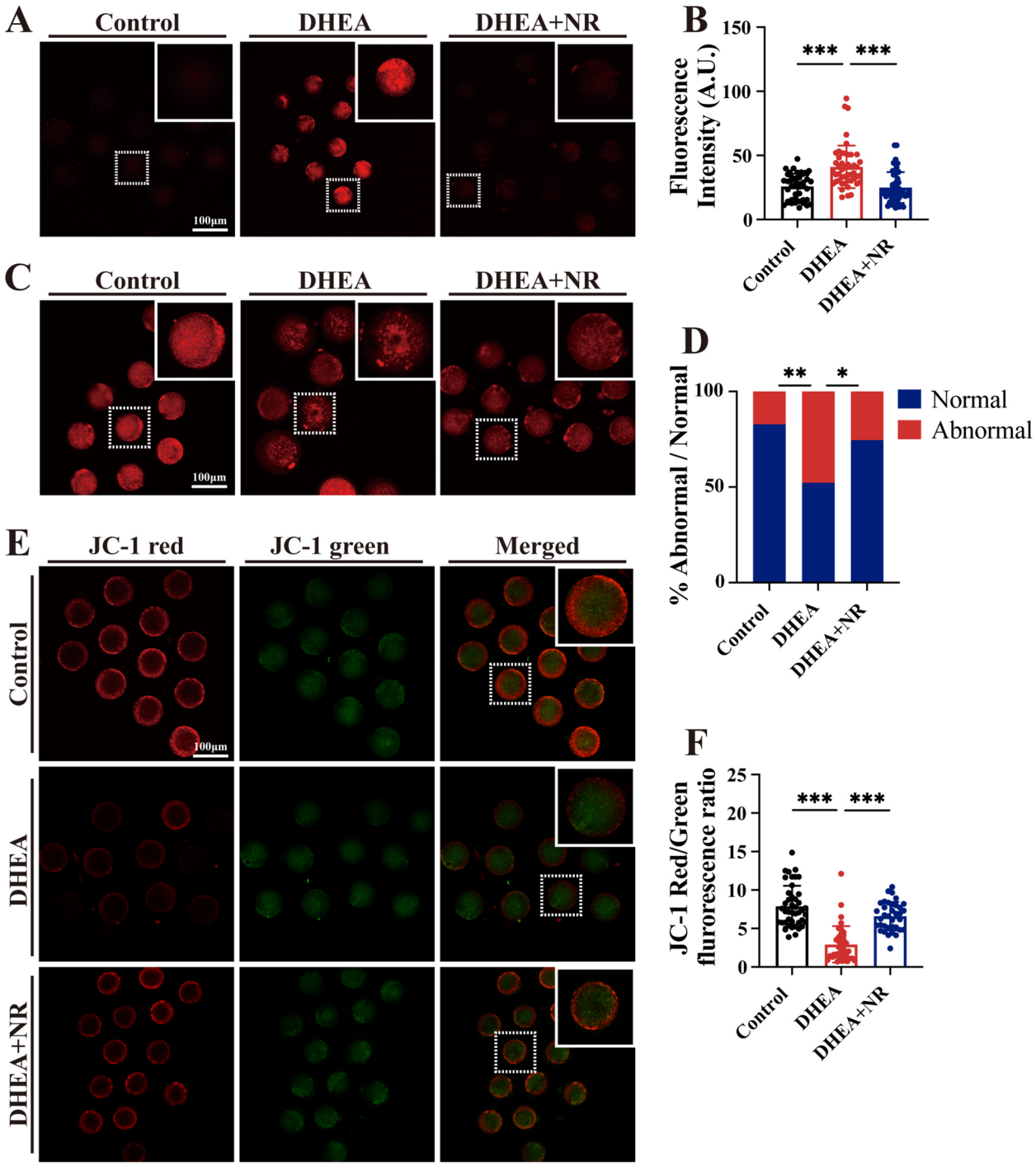

Fig. 2 NR supplementation reduced ROS levels and improved mitochondrial function in oocytes from PCOS mice. **A** Representative images of ROS levels in MII oocytes from three groups of mice determined by MitoSOX staining. Scale bar, 100 μm. **B** The fluorescence intensity of MitoSOX staining in oocytes from three groups of mice ($n = 44$ to 50 oocytes from 4 mice for each group). **C** Representative images of mitochondrial distribution in MII oocytes from three groups of mice determined by MitoTracker staining. Scale bar, 100 μm. **D** Percentages of abnormal mitochondrial distribution in MII oocytes from three groups of mice ($n = 43$ to 72 oocytes from 4 mice for each group). **E** Representative images of mitochondrial membrane potential in MII oocytes from three groups of mice determined by JC-1 staining. Scale bar, 100 μm. **F** Mitochondrial membrane potential in MII oocytes from three groups of mice evaluated by the ratio of red to green fluorescent pixels (n = 36 to 43 oocytes from 4 mice for each group). Data are presented as the mean ± SD. *$P < 0.05$, **$P < 0.01$, and ***$P < 0.001$ by one-way ANOVA compared to DHEA-treated mice

ovarian sections using anti-α smooth muscle actin antibody. Consistently, fibrosis was exacerbated in DHEA-treated mice, as evidenced by stronger staining intensity (Fig. 4C and D), which was alleviated by NR supplementation (Fig. 4C and D). Furthermore, we examined the mRNA expression levels of sirtuins and TGF-β signaling pathway-related genes in the ovaries of the three groups of mice. Compared to controls, the expression levels of *Sirt1* and *Sirt3* were significantly downregulated (Fig. 4E), while the expression levels of *Tgfb1* and *Smad3* were upregulated in DHEA-induced PCOS mice (Fig. 4E). NR supplementation effectively upregulated the expression of *Sirt1* and *Sirt3* and suppressed the expression of *Tgfb1* and *Smad3* (Fig. 4E), suggesting that NR supplementation may alleviate ovarian stromal fibrosis by activating *Sirt1* and *Sirt3* and inhibiting the TGF-β signaling pathway in PCOS. We further isolated ovarian stromal cells (Fig. 4F-H) and found, for the first time, that NAD^+ levels in these cells were decreased in PCOS mice compared to controls (Fig. 4I). NR supplementation increased NAD^+ levels in ovarian stromal cells from PCOS mice (Fig. 4I). Additionally, we assessed the expression levels of fibrosis-associated genes in ovarian stromal cells from three groups using qRT-PCR. Quantitative analysis showed that collagen-encoding genes *Col1a1*, *Col1a2*, and *Col3a1* were upregulated in the ovarian stromal cells from PCOS mice compared to controls (Fig. 4J-L). However, NR supplementation in PCOS mice decreased the expression levels of these genes in ovarian stromal cells (Fig. 4J-L). These results suggested that NR supplementation could reduce ovarian fibrosis and restore NAD^+ levels in ovarian stromal cells, thereby downregulating the expression of fibrosis-associated genes in PCOS mice.

NR supplementation improved mitochondrial function in ovarian stromal cells of PCOS mice

Based on the observed decrease in NAD^+ levels in ovarian stromal cells of PCOS mice, we next assessed the ROS content and mitochondrial membrane potential of ovarian stromal cells from three groups of mice by MitoSOX and JC-1 staining, respectively. The percentage of positive cells in ovarian stromal cells from PCOS mice detected by FCM was about 3.9 times higher compared to controls (Fig. 5A and B), indicating an elevation in ROS content in ovarian stromal cells of PCOS mice. However, following NR supplementation, the percentage of positive ovarian stromal cells in PCOS mice decreased by approximately 50% (Fig. 5A and B), indicating that NR supplementation effectively reduced ROS content in ovarian stromal cells of PCOS mice. Additionally, the red/green ratio of JC-1 staining in ovarian stromal cells from DHEA-treated mice evaluated by FCM showed a significant reduction compared to controls (Fig. 5C and D), while supplementation with NR increased the mitochondrial membrane potential (Fig. 5C and D), indicating that NR supplementation could alleviate mitochondrial dysfunction in the ovarian stromal cells from PCOS mice. These results suggested that mitochondrial defects in ovarian stroma cells might be an important driver in PCOS-related ovarian fibrosis. NR supplementation could alleviate ovarian fibrosis by improving mitochondrial function in ovarian stroma cells.

Discussion

PCOS is a significant gynecological endocrine condition distinguished by disturbances in follicular development and a reduction in the quality of oocytes, which is prevalent among women of reproductive age [45]. However, treatment strategies for improving oocyte quality are limited [2]. Here, we found that NR supplementation reduced the decline in NAD^+ levels and maintained the NAD^+/NADH redox balance in the ovaries of DHEA-induced PCOS mice. NR supplementation ameliorated ovarian dysfunction in PCOS mice, as evidenced by increased oocyte quantity and quality, reduced oocyte oxidative stress, improved oocyte mitochondrial function, and enhanced early embryonic development potential. Furthermore, NR supplementation mitigated ovarian fibrosis in PCOS mice by improving mitochondrial function in ovarian stromal cells, potentially elucidating the observed improvement in ovulation in PCOS mice following NR supplementation.

NAD^+ serves as a crucial cofactor for enzymes and plays an essential role in cellular energy metabolism and diverse metabolic pathways [46–48]. In this study, we observed that NAD^+ levels were reduced in the ovaries of

(See figure on next page.)

Fig. 3 NR supplementation alleviated spindle defects and improved embryonic development potential in PCOS mice. **A** Representative images of spindle morphology and chromosome alignment of MII oocytes from three groups of mice. Staining with anti-α-tubulin antibodies (green) was used to visualize the spindles, and DAPI (Blue) was used for chromosome localization. Scale bar, 20 μm. **B** The rates of MII oocytes with abnormal spindles from three groups of mice ($n = 5$ mice for each group). **C** Representative images of 2-cell embryos, 4-cell embryos, morula, and blastocyst from three groups of mice. Scale bar, 100 μm. **D** The rates of 2-cell embryos and (**E**) blastocyst formation from three groups of mice ($n = 4$ to 6 mice for each group). Data are presented as the mean ± SD. $^*P < 0.05$, $^{**}P < 0.01$, and $^{***}P < 0.001$ by one-way ANOVA compared to DHEA-treated mice

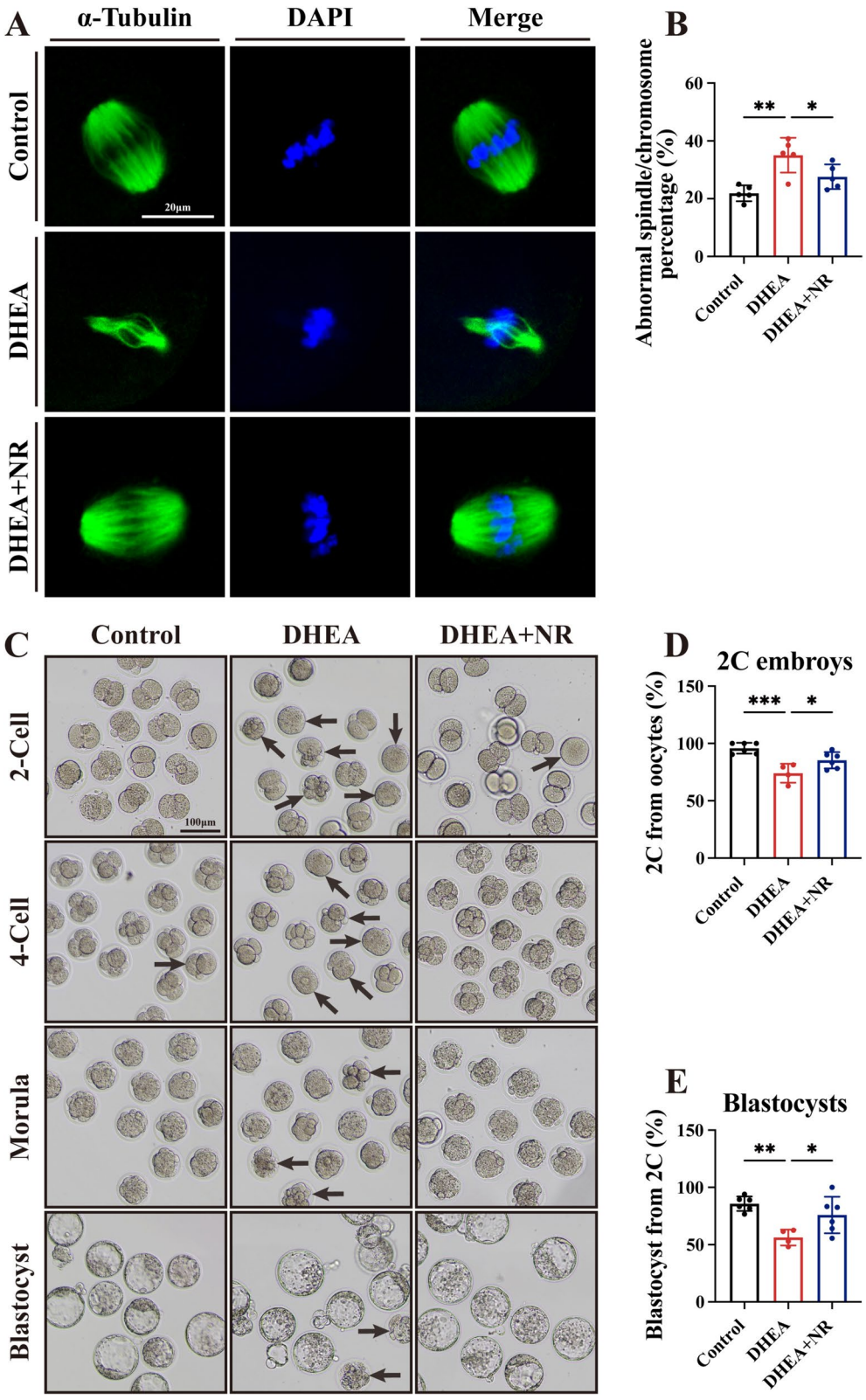

Fig. 3 (See legend on previous page.)

PCOS mice compared to controls. However, supplementation with NR increased ovarian NAD^+ levels in PCOS mice. Notably, one study reported an increase in liver NAD^+ levels in DHEA-treated male rats [49]. Another study demonstrated a decrease in muscle NAD^+ levels in DHT-induced PCOS mice, which was normalized by NMN supplementation [50], indicating that the effect of DHEA on NAD^+ levels may vary across different organs. NAD predominantly exists in two forms in cells: NAD^+ and NADH [51, 52]. NADH is a critical intermediate in converting chemical energy to ATP in the mitochondria, while NAD^+ promotes redox reactions. The levels of NAD^+ directly influence redox reactions, while the ratio of NAD^+/NADH is crucial for maintaining mitochondrial function and overall cellular health [53–55]. DHEA inhibits the pentose phosphate pathway (PPP), reducing the production of NADPH and affecting NADH generation [56]. Here, we observed a decreased ovarian NAD^+/NADH ratio in PCOS mice. In contrast, NR supplementation increased the ovarian NAD^+/NADH ratio in PCOS mice. These results collectively indicated that NR supplementation may mitigate the decrease in NAD^+ levels and maintain the NAD^+/NADH redox balance in the ovaries of PCOS mice. Whether DHEA affects NAD^+ synthesis or consumption needs further investigation in future studies. In addition, our previous research observed reduced NAD^+ levels in LPS-treated KGN cells [22], highlighting a potential link between inflammation and NAD^+ metabolism. Future studies could further investigate the effects of inflammation on NAD^+ levels and redox balance by treating animal models with LPS.

NR supplementation improves NAD^+ biosynthesis and cellular metabolism [32, 57], which has been shown to improve female fertility, particularly in aged individuals [26, 34]. NMN supplementation has been shown to normalize the aberrant metabolic features observed in DHT-induced PCOS mice, including hyperinsulinemia, obesity, and hepatic lipid accumulation [50], suggesting that NR supplementation may also alleviate organ damage associated with PCOS. In this study, we observed a decrease in ovarian ATP levels in DHEA-treated mice compared to controls, while NR supplementation significantly increased ovarian ATP levels. Additionally, NR supplementation upregulated the mRNA expression levels of mitochondrial complex-related genes in the ovaries of DHEA-treated mice. These findings collectively suggest that NR supplementation could improve mitochondrial function and energy metabolism in the ovaries of DHEA-induced PCOS mice.

Infertility associated with PCOS is primarily characterized by anovulation due to abnormal follicular development and ovulatory dysfunction [58], which is manifested by menstrual cycle disorders accompanied by decreased oocyte quality [59, 60]. However, clinical treatments for infertility related to PCOS are still limited to lifestyle adjustments and ART [4, 5]. Here, we observed disrupted estrous cycles in PCOS mice, whereas NR supplementation alleviated estrous cycle irregularities in PCOS mice. Additionally, our study revealed a significant reduction in the number of ovulated oocytes in PCOS mice compared to controls. This decrease was also associated with a higher incidence of oocytes exhibiting morphological abnormalities. In contrast, NR supplementation improved the oocyte quantity and quality in PCOS mice. In addition, gonadotropin-treated ovary sections of PCOS mice often exhibited non-ovulated follicles, which were rarely observed in controls and NR-supplemented PCOS mice. These results suggested that supplementation with NR could improve PCOS-related ovulation disorders.

We next examined oocyte quality to investigate whether NR supplementation could mitigate mitochondrial dysfunction in PCOS mice. Consistent with previous studies [21, 61], oocytes from PCOS mice displayed impaired mitochondrial function, characterized by a higher percentage of MII oocytes with aberrant mitochondrial clusters and lower mitochondrial membrane potential. However, these mitochondrial defects in oocytes from PCOS mice were alleviated after NR supplementation. Elevated incidences of meiotic spindle abnormalities and aneuploidy in oocytes are contributing factors to infertility during reproductive aging [62]. Previous studies demonstrated that mitochondrial dysfunction and oxidative stress in oocytes were implicated

(See figure on next page.)

Fig. 4 Ovarian stromal fibrosis in PCOS mice was reduced by NR supplementation. **A** Representative images of ovarian collagen content in three groups of mice measured by PSR staining. Scale bar, 500 μm. **B** Quantitative analysis of fibrotic area in ovarian sections from three groups of mice ($n = 8$ to 13 slices for each group). **C** Representative images of ovarian fibrosis in the three groups of mice measured by immunohistochemistry. Scale bar, 500 μm. **D** Quantification of immunohistochemical staining intensity of ovarian sections from the three groups of mice ($n = 16$ slices for each group). **E** Transcriptional levels of *Sirt1*, *Sirt3*, *Tgfb1*, and *Smad3* genes in the ovaries were measured by qRT-PCR ($n = 3$ replicates from 3 mice). **F** Diagram of the isolation of ovarian stromal cells. **G**, **H** qRT-PCR was conducted to validate the purity of the isolation. **I** $NAD.^+$ levels in ovarian stromal cells ($n = 3$ replicates of cells pooled from 4 mice). **J** Transcript levels of *Col1a1*, (**K**) *Col1a2*, and (**L**) *Col3a1* genes in ovarian stromal cells detected by qRT-PCR (n = 3 replicates of cells pooled from 4 mice). Data are presented as the mean ± SD. $^*P < 0.05$, $^{**}P < 0.01$, and $^{***}P < 0.001$ by one-way ANOVA compared to DHEA-treated mice (B, F-I) or Student's *t*-test (**D**, **E**)

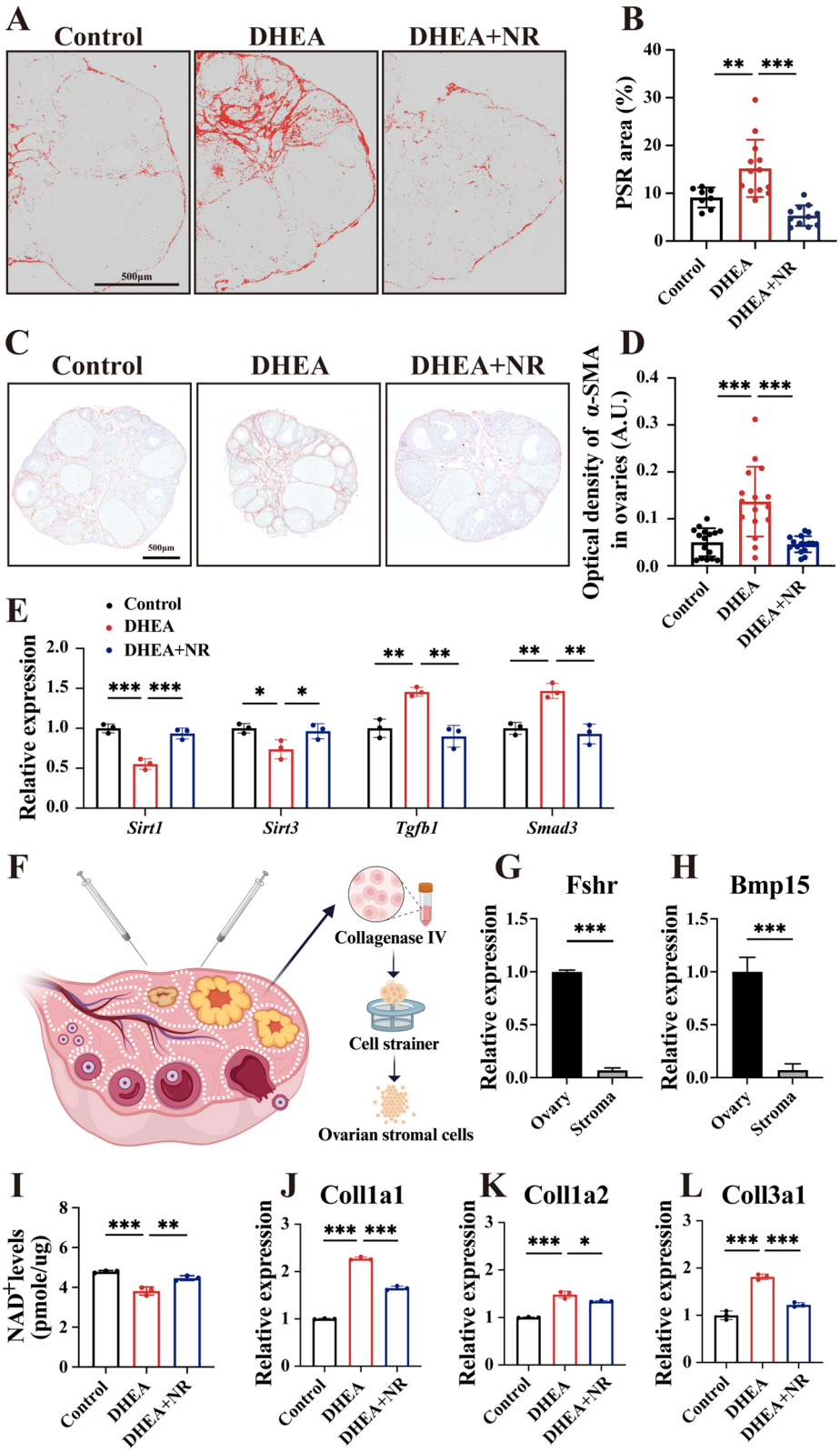

Fig. 4 (See legend on previous page.)

in the higher occurrence of spindle abnormalities and reduced embryo preimplantation potential [41, 63]. Consistently with other reports [28, 64], we also observed significantly elevated ROS levels as well as a higher rate of spindle abnormalities in oocytes from PCOS mice as compared to controls. However, increasing NAD^+ levels through NR supplementation significantly reduced ROS accumulation and improved spindle assembly in oocytes from PCOS mice. These findings were consistent with previous research indicating that NAD^+ acted as a scavenger of free radicals, thereby reducing oxidative stress [38, 65]. Furthermore, we also found that the rates of 2-cell embryos and blastocyst formation in oocytes postfertilization were decreased in PCOS mice compared to controls. As expected, NR supplementation increased the developmental capacity of early embryos in PCOS mice. Collectively, these results suggested that NAD^+ supplementing could improve ovarian function and early embryonic development potential in PCOS mice. This approach might represent a promising therapeutic strategy for addressing infertility associated with PCOS. Notably, in this study, we employed a DHEA-induced PCOS mouse model. However, the pathogenesis of polycystic ovary syndrome is highly complex. The clinical therapeutic potential of NR supplementation for PCOS requires further investigation, and dose–response testing as well as control groups for NR supplementation should be considered.

Fibrosis manifests through the excessive buildup of extracellular matrix (ECM) components, such as collagen and fibronectin [66]. Ovarian fibrosis appears to affect adjacent secondary follicles, resulting in compromised follicular development [67]. Antifibrosis drugs have been shown to degrade fibrotic collagen and subsequently restore ovulatory function in reproductively aged and obese mice [11]. In line with a previous study [10], we observed a significant increase in accumulated fibrillar collagen in the ovaries of PCOS mice compared to controls. Notably, NR supplementation effectively reduced this ovarian fibrosis. DHEA-induced ovarian fibrosis is mediated by the TGF-β signaling pathway [68]. Activation of *Sirt1* has been demonstrated to attenuate fibrosis by inhibiting the TGF-β pathway [69, 70]. Additionally, *Sirt3* has been reported to ameliorate PCOS by improving mitochondrial function [71]. Consistently, we showed that in the ovaries of DHEA-treated mice, the mRNA expression levels of *Sirt1* and *Sirt3* were significantly downregulated, whereas the expression levels of *Tgfb1* and *Smad3* were upregulated. In contrast, NR supplementation led to a significant upregulation of *Sirt1* and *Sirt3* expression, accompanied by a downregulation of *Tgfb1* and *Smad3*. These results suggested that NR supplementation may mitigate ovarian stromal fibrosis by activating Sirt1 and Sirt3 and modulating the TGF-β signaling pathway. For the first time, we found that ovarian stromal cells from PCOS mice exhibited lower NAD^+ levels compared to controls. NR supplementation significantly increased these NAD^+ levels in PCOS mice. Furthermore, we revealed upregulation of collagen-encoding genes *Col1a1*, *Col1a2*, and *Col3a1* in ovarian stromal cells of PCOS mice compared to controls. However, NR supplementation led to the downregulation of these fibrosis-related genes in PCOS mice. We next evaluated ROS levels and mitochondrial membrane potential in ovarian stromal cells from the three groups of mice. Consistent with previous studies [68, 72, 73], we observed significantly elevated levels of ROS in ovarian stromal cells of PCOS mice, along with reduced mitochondrial membrane potential. However, NR supplementation significantly reduced ROS levels and increased mitochondrial membrane potential in ovarian stromal cells of PCOS mice. These results indicated that supplementation with NR effectively alleviated ovarian fibrosis in PCOS mice by alleviating oxidative stress and improving mitochondrial function in ovarian stromal cells, potentially elucidating the observed improvement in ovulation of PCOS mice after NR supplementation.

In summary, we identified a deficiency in NAD^+ levels and disrupted NAD^+ metabolism in the ovaries of PCOS mice. NR supplementation effectively improved mitochondrial function by increasing NAD^+ levels and maintaining the NAD^+/NADH redox balance, leading to increased oocyte quantity and quality and enhanced early embryonic development potential in PCOS mice. Additionally, NR supplementation alleviated ovarian fibrosis in PCOS mice by improving mitochondrial function in ovarian stromal cells, potentially explaining the improved ovulatory function in NR-supplemented PCOS mice.

(See figure on next page.)

Fig. 5 NR supplementation decreased ROS levels and increased mitochondrial membrane potential in ovarian stromal cells of PCOS mice. **A** Ovarian stromal cells from three groups of mice were stained with MitoSOX to assess ROS levels using FCM. **B** The percentages of ovarian stromal cells with high ROS levels ($n = 9$–15 replicates of cells pooled from 3 mice). **C** Ovarian stromal cells from three groups of mice were stained with JC-1 to assess mitochondrial membrane potential using FCM. The x-axis represents JC-1 green fluorescence, while the y-axis represents JC-1 red fluorescence. **D** The ratios of red to green fluorescence in ovarian stromal cells ($n = 11$ replicates of cells pooled from 3 mice). Data are presented as the mean ± SD. $^{**}P < 0.01$ and $^{***}P < 0.001$ by one-way ANOVA compared to DHEA-treated mice

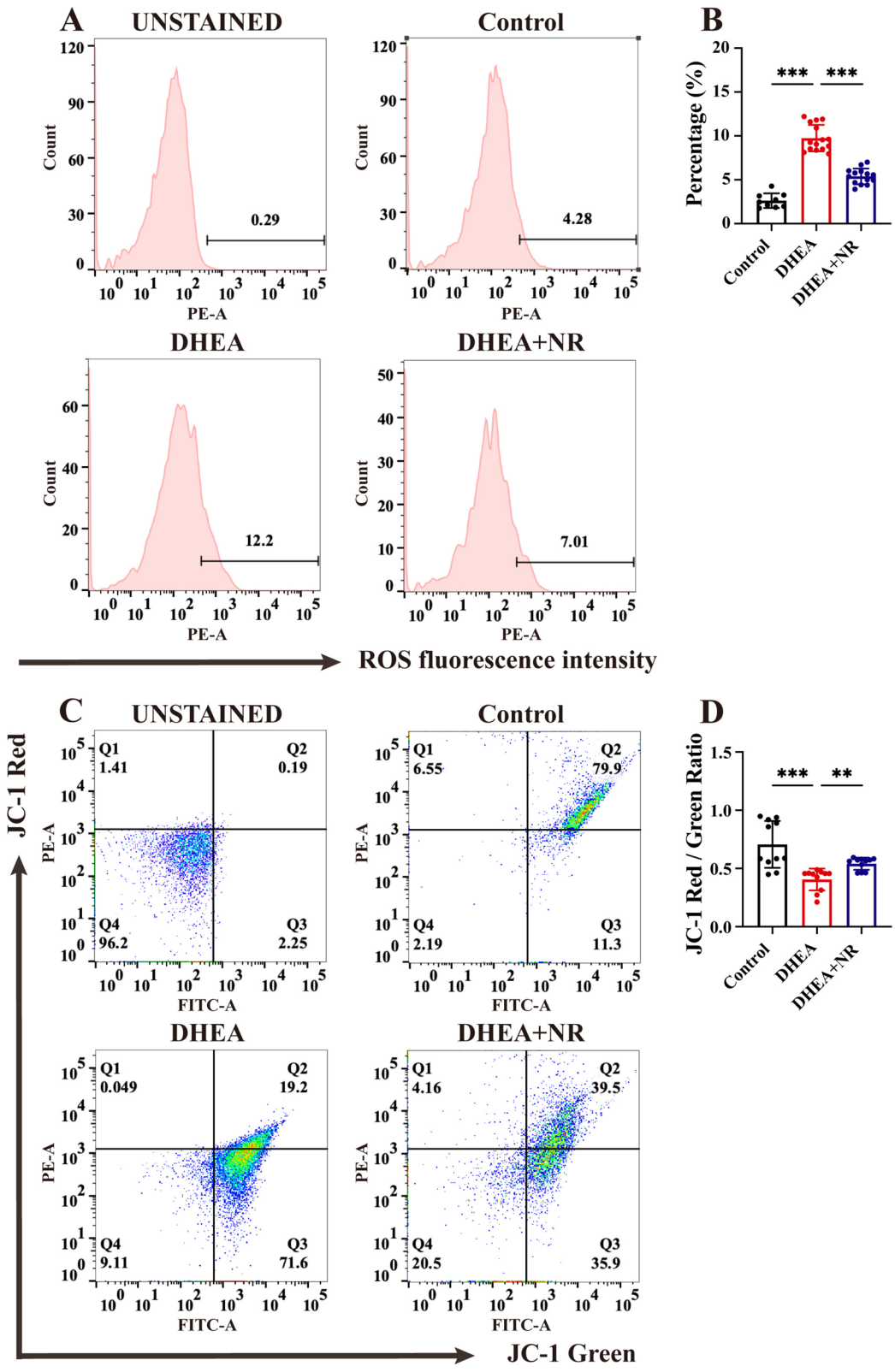

Fig. 5 (See legend on previous page.)

These findings not only provided novel insights into the role of NAD^+ in PCOS but also laid the foundation for the potential clinical application of NR in ameliorating ovarian dysfunction in women with PCOS.

It is worth noting that although our results suggest that NR can improve cellular metabolism and alleviate PCOS phenotypes in mice, the observed improvements in this study may also be partially attributed to natural recovery after the discontinuation of DHEA injections. Future studies are needed to further clarify the specific role of NR supplementation in improving PCOS phenotypes. Additionally, the relationship between the duration of DHEA treatment and the induced ovarian fibrosis warrants further investigation in future work.

Abbreviations

PCOS	Polycystic ovary syndrome
NAD^+	Nicotinamide adenine dinucleotide
GCs	Granulosa cells
ROS	Reactive oxygen species
NR	Nicotinamide riboside
DHEA	Dehydroepiandrosterone
ART	Assisted reproductive technologies
KGN	Human granulosa-like tumor cell line
LPS	Lipopolysaccharide
DHT	Dihydrotestosterone
COCs	Cumulus-oocyte complexes
MII	Metaphase II
IVF	in vitro Fertilization
PSR	Picrosirius red
ATP	Adenosine triphosphate
ECM	Extracellular matrix
PPP	Pentose phosphate pathway

Supplementary Information

The online version contains supplementary material available at https://doi.org/10.1186/s13048-025-01596-4.

Supplementary Material 1.

Acknowledgements
Not applicable.

Authors' contributions
Y.P. Sun and Q.L. Yang designed the study and provided funding support. Q.L. Yang and Z.Y. Zhu contributed to data interpretation and manuscript writing. Z.Y. Zhu, M. Lei, and R.Z. Guo participated in the construction of the mouse model and experimental work. Y.N. Xu, Y.Q. Zhao and C.L. Wei provided technical support for the related experiments.

Funding
This work was supported by the National Key R&D Program of China (2019YFA0110900), key international (regional) cooperative research projects of China (81820108016), the National Natural Science Foundation of China (31970800 and 32370917), and Funding for Scientific Research and Innovation Team of The First Affiliated Hospital of Zhengzhou University (QNCXTD2023017).

Data availability
No datasets were generated or analysed during the current study.

Declarations

Ethics approval and consent to participate
The current study received ethical approval, and all animal experiments were conducted in compliance with the regulations and guidelines of the ethics committee of the First Affiliated Hospital of Zhengzhou University.

Consent for publication
Not applicable.

Competing interests
The authors declare no competing interests.

Author details
[1]Center for Reproductive Medicine, The First Affiliated Hospital of Zhengzhou University, Zhengzhou 450052, China. [2]Henan Key Laboratory of Reproduction and Genetics, The First Affiliated Hospital of Zhengzhou University, Zhengzhou, China. [3]Henan Provincial Obstetrical and Gynecological Diseases (Reproductive Medicine) Clinical Research Center, The First Affiliated Hospital of Zhengzhou University, Zhengzhou, China.

Received: 19 September 2024 Accepted: 9 January 2025
Published online: 20 January 2025

References

1. Azziz R, et al. The prevalence and features of the polycystic ovary syndrome in an unselected population. J Clin Endocrinol Metab. 2004;89(6):2745–9.
2. Rababa'h AM, Matani BR, Yehya A. An update of polycystic ovary syndrome: causes and therapeutics options. Heliyon. 2022;8(10):e11010.
3. Franks S, Stark J, Hardy K. Follicle dynamics and anovulation in polycystic ovary syndrome. Hum Reprod Update. 2008;14(4):367–78.
4. Cunha A, Póvoa AM. Infertility management in women with polycystic ovary syndrome: a review. Porto Biomed J. 2021;6(1):e116.
5. Melo AS, Ferriani RA, Navarro PA. Treatment of infertility in women with polycystic ovary syndrome: approach to clinical practice. Clinics (Sao Paulo). 2015;70(11):765–9.
6. Murri M, et al. Circulating markers of oxidative stress and polycystic ovary syndrome (PCOS): a systematic review and meta-analysis. Hum Reprod Update. 2013;19(3):268–88.
7. Victor VM, et al. Insulin resistance in pcos patients enhances oxidative stress and leukocyte adhesion: role of myeloperoxidase. PLoS ONE. 2016;11(3):e0151960.
8. Rudnicka E, et al. Chronic low grade inflammation in pathogenesis of PCOS. Int J Mol Sci. 2021;22(7):3789.
9. Aboeldalyl S, et al. The role of chronic inflammation in polycystic ovarian syndrome-a systematic review and meta-analysis. Int J Mol Sci. 2021;22(5):2734.
10. Hughesdon PE. Morphology and morphogenesis of the Stein-Leventhal ovary and of so-called "hyperthecosis." Obstet Gynecol Surv. 1982;37(2):59–77.
11. Umehara T, et al. Female reproductive life span is extended by targeted removal of fibrotic collagen from the mouse ovary. Sci Adv. 2022;8(24):eabn4564.
12. Landry DA, et al. Metformin prevents age-associated ovarian fibrosis by modulating the immune landscape in female mice. Sci Adv. 2022;8(35):eabq1475.
13. Briley SM, et al. Reproductive age-associated fibrosis in the stroma of the mammalian ovary. Reproduction. 2016;152(3):245–60.
14. Snider AP, Wood JR. Obesity induces ovarian inflammation and reduces oocyte quality. Reproduction. 2019;158(3):R79-r90.
15. Zong Y, et al. Mitochondrial dysfunction: mechanisms and advances in therapy. Signal Transduct Target Ther. 2024;9(1):124.
16. Filomeni G, De Zio D, Cecconi F. Oxidative stress and autophagy: the clash between damage and metabolic needs. Cell Death Differ. 2015;22(3):377–88.

17. Chen W, Zhao H, Li Y. Mitochondrial dynamics in health and disease: mechanisms and potential targets. Signal Transduct Target Ther. 2023;8(1):333.
18. Yuan Z, et al. Extracellular matrix remodeling in tumor progression and immune escape: from mechanisms to treatments. Mol Cancer. 2023;22(1):48.
19. Taddei ML, et al. Mitochondrial oxidative stress due to complex I dysfunction promotes fibroblast activation and melanoma cell invasiveness. J Signal Transduct. 2012;2012:684592.
20. Siemers KM, Klein AK, Baack ML. Mitochondrial dysfunction in PCOS: insights into reproductive organ pathophysiology. Int J Mol Sci. 2023;24(17):13123.
21. Zhang Q, et al. Mitochondrial and glucose metabolic dysfunctions in granulosa cells induce impaired oocytes of polycystic ovary syndrome through Sirtuin 3. Free Radic Biol Med. 2022;187:1–16.
22. Wang Y, et al. NAD+ deficiency and mitochondrial dysfunction in granulosa cells of women with polycystic ovary syndrome‡. Biol Reprod. 2021;105(2):371–80.
23. Cantó C, Menzies KJ, Auwerx J. NAD(+) metabolism and the control of energy homeostasis: A balancing act between mitochondria and the nucleus. Cell Metab. 2015;22(1):31–53.
24. Amjad S, et al. Role of NAD(+) in regulating cellular and metabolic signaling pathways. Mol Metab. 2021;49:101195.
25. Camacho-Pereira J, et al. CD38 dictates age-related nad decline and mitochondrial dysfunction through an SIRT3-dependent mechanism. Cell Metab. 2016;23(6):1127–39.
26. Yang Q, et al. Increasing ovarian NAD(+) levels improve mitochondrial functions and reverse ovarian aging. Free Radic Biol Med. 2020;156:1–10.
27. Poljšak B, et al. The central role of the NAD+ molecule in the development of aging and the prevention of chronic age-related diseases: strategies for NAD+ modulation. Int J Mol Sci. 2023;24(3):2959.
28. Li T, et al. Tempol ameliorates polycystic ovary syndrome through attenuating intestinal oxidative stress and modulating of gut microbiota composition-serum metabolites interaction. Redox Biol. 2021;41:101886.
29. Teng X, Wang Z, Wang X. Enhancing angiogenesis and inhibiting apoptosis: evaluating the therapeutic efficacy of bone marrow mesenchymal stem cell-derived exosomes in a DHEA-induced PCOS mouse model. J Ovarian Res. 2024;17(1):121.
30. Xie Q, et al. Mesenchymal stem cells alleviate DHEA-Induced Polycystic Ovary Syndrome (PCOS) by inhibiting inflammation in mice. Stem Cells Int. 2019;2019:9782373.
31. Nascimento EBM, et al. Nicotinamide riboside enhances in vitro beta-adrenergic brown adipose tissue activity in humans. J Clin Endocrinol Metab. 2021;106(5):1437–47.
32. Cantó C, et al. The NAD(+) precursor nicotinamide riboside enhances oxidative metabolism and protects against high-fat diet-induced obesity. Cell Metab. 2012;15(6):838–47.
33. Yang Q, et al. Deletion of enzymes for de novo NAD(+) biosynthesis accelerated ovarian aging. Aging Cell. 2023;22(9):e13904.
34. Yang Q, et al. NAD(+) repletion attenuates obesity-induced oocyte mitochondrial dysfunction and offspring metabolic abnormalities via a SIRT3-dependent pathway. Clin Transl Med. 2021;11(12):e628.
35. Ajayi AF, Akhigbe RE. Staging of the estrous cycle and induction of estrus in experimental rodents: an update. Fertil Res Pract. 2020;6:5.
36. Zeber-Lubecka N, Ciebiera M, Hennig EE. Polycystic ovary syndrome and oxidative stress-from bench to bedside. Int J Mol Sci. 2023;24(18):14126.
37. Murphy MP. How mitochondria produce reactive oxygen species. Biochem J. 2009;417(1):1–13.
38. Guo C, et al. Oxidative stress, mitochondrial damage and neurodegenerative diseases. Neural Regen Res. 2013;8(21):2003–14.
39. Bhatti JS, Bhatti GK, Reddy PH. Mitochondrial dysfunction and oxidative stress in metabolic disorders - A step towards mitochondria based therapeutic strategies. Biochim Biophys Acta Mol Basis Dis. 2017;1863(5):1066–77.
40. Perkins AT, et al. Oxidative stress in oocytes during midprophase induces premature loss of cohesion and chromosome segregation errors. Proc Natl Acad Sci U S A. 2016;113(44):E6823-e6830.
41. D'Angiolella V, Santarpia C, Grieco D. Oxidative stress overrides the spindle checkpoint. Cell Cycle. 2007;6(5):576–9.
42. Wan Y, et al. IGF2 reduces meiotic defects in oocytes from obese mice and improves embryonic developmental competency. Reprod Biol Endocrinol. 2022;20(1):101.
43. Munné S. Chromosome abnormalities and their relationship to morphology and development of human embryos. Reprod Biomed Online. 2006;12(2):234–53.
44. Takahashi N, et al. Activation of endoplasmic reticulum stress in granulosa cells from patients with polycystic ovary syndrome contributes to ovarian fibrosis. Sci Rep. 2017;7(1):10824.
45. Norman RJ, et al. Polycystic ovary syndrome. Lancet. 2007;370(9588):685–97.
46. Ruskovska T, Bernlohr DA. The role of NAD(+) in metabolic regulation of adipose tissue: implications for obesity-induced insulin resistance. Biomedicines. 2023;11(9):2560.
47. Xu Q, et al. Mechanism research and treatment progress of NAD pathway related molecules in tumor immune microenvironment. Cancer Cell Int. 2022;22(1):242.
48. Lautrup S, et al. NAD(+) in brain aging and neurodegenerative disorders. Cell Metab. 2019;30(4):630–55.
49. Swierczyński J, et al. Increase in NAD but not ATP and GTP concentrations in rat liver by dehydroepiandrosterone feeding. Pol J Pharmacol. 2001;53(2):125–30.
50. Aflatounian A, et al. Declining muscle NAD(+) in a hyperandrogenism PCOS mouse model: Possible role in metabolic dysregulation. Mol Metab. 2022;65:101583.
51. Walker MA, Tian R. NAD(H) in mitochondrial energy transduction: implications for health and disease. Curr Opin Physiol. 2018;3:101–9.
52. Stein LR, Imai S. The dynamic regulation of NAD metabolism in mitochondria. Trends Endocrinol Metab. 2012;23(9):420–8.
53. Liang J, et al. Impact of NAD+ metabolism on ovarian aging. Immun Ageing. 2023;20(1):70.
54. Yuan X, et al. NAD(+)/NADH redox alterations reconfigure metabolism and rejuvenate senescent human mesenchymal stem cells in vitro. Commun Biol. 2020;3(1):774.
55. Hu Q, et al. Genetically encoded biosensors for evaluating NAD(+)/NADH ratio in cytosolic and mitochondrial compartments. Cell Rep Methods. 2021;1(7):100116.
56. Schwartz AG, Pashko LL. Dehydroepiandrosterone, glucose-6-phosphate dehydrogenase, and longevity. Ageing Res Rev. 2004;3(2):171–87.
57. Canto C. NAD(+) precursors: a questionable redundancy. Metabolites. 2022;12(7):630.
58. Witchel SF, Oberfield SE, Peña AS. Polycystic ovary syndrome: pathophysiology, presentation, and treatment with emphasis on adolescent girls. J Endocr Soc. 2019;3(8):1545–73.
59. Danfeng D, et al. Oocyte quality is impaired in a hyperandrogenic PCOS mouse model by increased Foxo1 expression. Reprod Biol. 2023;23(4):100812.
60. Balen AH, et al. The management of anovulatory infertility in women with polycystic ovary syndrome: an analysis of the evidence to support the development of global WHO guidance. Hum Reprod Update. 2016;22(6):687–708.
61. Shukla P, Mukherjee S. Mitochondrial dysfunction: an emerging link in the pathophysiology of polycystic ovary syndrome. Mitochondrion. 2020;52:24–39.
62. Selesniemi K, et al. Prevention of maternal aging-associated oocyte aneuploidy and meiotic spindle defects in mice by dietary and genetic strategies. Proc Natl Acad Sci U S A. 2011;108(30):12319–24.
63. Zhang X, et al. Deficit of mitochondria-derived ATP during oxidative stress impairs mouse MII oocyte spindles. Cell Res. 2006;16(10):841–50.
64. Rajani S, et al. Assessment of oocyte quality in polycystic ovarian syndrome and endometriosis by spindle imaging and reactive oxygen species levels in follicular fluid and its relationship with IVF-ET outcome. J Hum Reprod Sci. 2012;5(2):187–93.
65. Massudi H, et al. NAD+ metabolism and oxidative stress: the golden nucleotide on a crown of thorns. Redox Rep. 2012;17(1):28–46.
66. Henderson NC, Rieder F, Wynn TA. Fibrosis: from mechanisms to medicines. Nature. 2020;587(7835):555–66.

67. Umehara T, Richards JS, Shimada M. The stromal fibrosis in aging ovary. Aging (Albany NY). 2018;10(1):9–10.
68. Wang D, et al. DHEA-induced ovarian hyperfibrosis is mediated by TGF-β signaling pathway. J Ovarian Res. 2018;11(1):6.
69. Huang XZ, et al. Sirt1 activation ameliorates renal fibrosis by inhibiting the TGF-β/Smad3 pathway. J Cell Biochem. 2014;115(5):996–1005.
70. Zhou J, et al. Paeoniflorin attenuates DHEA-induced polycystic ovary syndrome via inactivation of TGF-β1/Smads signaling pathway in vivo. Aging (Albany NY). 2021;13(5):7084–95.
71. Pang X, et al. SIRT3 ameliorates polycystic ovary syndrome through FOXO1/PGC-1α signaling pathway. Endocrine. 2023;80(1):201–11.
72. Huang T, et al. Efficient intervention for pulmonary fibrosis via mitochondrial transfer promoted by mitochondrial biogenesis. Nat Commun. 2023;14(1):5781.
73. Li X, et al. Mitochondrial dysfunction in fibrotic diseases. Cell Death Discov. 2020;6:80.

Publisher's Note